社団法人　電子情報通信学会
THE INSTITUTE OF ELECTRONICS,
INFORMATION AND COMMUNICATION ENGINEERS

信学技報
TECHNICAL REPORT OF IEICE.

Research on Clustering of Coupled Chaotic Circuits with Mutual Inductors

Yuta KOMATSU†, Yoko UWATE†, and Yoshifumi NISHIO†

† Department of Electrical and Electronic Engineering, Tokushima University
2-1 Minami-Josanjima, Tokushima, Japan
E-mail: †{komatsu, uwate, nishio}@ee.tokushima-u.ac.jp

Abstract In this study, the clustering phenomenon observed from chaotic circuits coupled by mutual inductors is investigated. In order to analyze the phenomena, dependent variables corresponding to phases of solutions for subcircuits are introduced. By using this dependent variables, we make detailed investigation on the statistical information of the clustering for a six subcircuit case, such as sojourn time of a certain size of clusters, the number of clusters, and so on.

Key words Chaotic Circuit, Clustering, Mutual Inductor

1. Introduction

Clustering is one of the most interesting nonlinear phenomena observed from a large number of coupled chaotic systems. A lot of studies on the clustering have been carried out for discrete-time mathematical models [1][2]. However, there have been a few studies on clustering of continuous-time real physical systems such as electrical circuits [3][4].

In our previous study, quasi-synchronization phenomena observed from chaotic circuits coupled by mutual inductors were investigated [5]. We could observe various kinds of synchronization phenomena of chaos by carrying out computer calculations and circuit experiments for two or three subcircuit cases. However, we could not investigate the complex phenomena observed from higher dimensional circuits such as clustering, chaotic wandering, pattern switching, and so on.

In this study, we focus on the clustering phenomenon. We investigate the clustering observed from chaotic circuits coupled by mutual inductors in detail. By computer calculations, the generation of clustering and chaotic changings of the synchronization states are confirmed. In order to analyze the phenomena, dependent variables corresponding to phases of solutions for subcircuits are introduced. By using this dependent variables, we make detailed investigation on the statistical information of the clustering for a six subcircuit case, such as sojourn time of a certain size of clusters, the number of clusters, and so on.

2. Circuit Model

Figure 1 shows the circuit model. In the circuit, N identical chaotic circuits are coupled symmetrically by mutual inductors. Each chaotic subcircuit is a symmetric version of the circuit model proposed by Inaba *et al.* [6]. It consists of three memory elements, one linear negative resistor and one nonlinear resistor, and is one of the simplest autonomous chaotic circuits. First, we approximate the $i-v$ characteristics of the nonlinear resistor consisting of diodes by the following function.

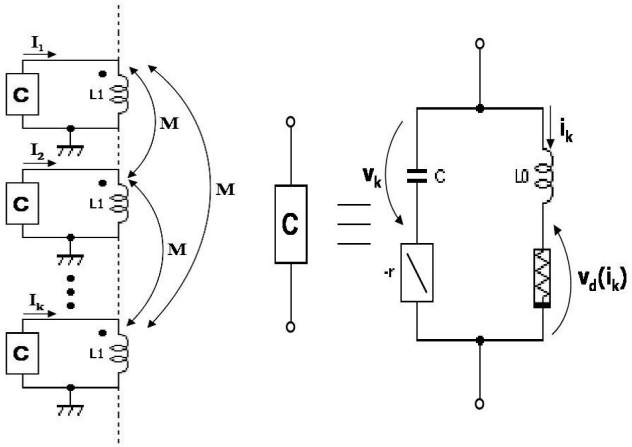

Fig. 1　Circuit model.

$$v_d(i_k) = \sqrt[9]{r_d\, i_k}. \tag{1}$$

By changing the variables and parameters,

$$t = \sqrt{(L_1 - M)\,C}\,\tau, \quad a = \sqrt[8]{r_d \frac{C}{L_1 - M}}, \quad \text{“}\cdot\text{”} = \frac{d}{d\tau},$$
$$I_k = a\sqrt{\frac{C}{L_1 - M}}\,x_k, \quad i_k = a\sqrt{\frac{C}{L_1 - M}}\,y_k, \quad v_k = a z_k,$$
$$\alpha = \frac{L_1 - M}{L_2}, \quad \beta = r\sqrt{\frac{C}{L_1 - M}}, \quad \gamma = \frac{M}{L_1}. \tag{2}$$

the circuit equations are normalized and described as

$$\begin{aligned}\dot{x}_k &= \beta(x_k + y_k) - z_k \\ &\quad - \frac{\gamma}{1+(N-1)\gamma}\sum_{j=1}^{N}\{\beta(x_j + y_j) - z_j\} \\ \dot{y}_k &= \alpha\{\beta(x_k + y_k) - z_k - f(y_k)\} \\ \dot{z}_k &= x_k + y_k \qquad\qquad (k = 1, 2, \cdots, N)\end{aligned} \tag{3}$$

where

$$f(y_k) = \sqrt[3]{y_k}. \tag{4}$$

In the following computer calculations, (3) is calculated by using the Runge-Kutta method with step size $\Delta t = 0.005$.

3. Clustering Phenomenon

We carried out computer calculations for the case of $N = 6$. Figure 2 shows computer calculated results. Upper and lower figures in Fig. 2 show phase differences. While, middle figures show attractors. From Fig. 2, we can confirm the generation of the clustering phenomenon and chaotic changings of the synchronization states. In Fig. 2(a), subcircuit 1 is synchronized at the in-phase in almost all of the times and sometimes becomes the asynchronous state for subcircuits 3 and 6. While, for subcircuits 2, 4, and 5, subcircuit 1 becomes the anti-phase syncronization state in almost all of the times and the asynchronous state occasionally. As we can see from this figure, a size of the cluster for subcircuit 1 is principally 3 under these parameters.

By changing the parameter β, the switching phenomenon can be confirmed at $\tau = 2500, 5000$ as shown in Fig. 2(b). In the interval [0, 2500], subcircuit 1 is almost synchronized with subcircuits 2, 4 and 5 at the anti-phase, and almost becomes the in-phase synchronization state for subcircuits 3 and 6. Moreover, the size of the cluster that subcircuit 1 belongs to is principally 3 in this interval. While, subcircuit 1 becomes the in-phase synchronization state for subcircuit 2 in the interval [2500, 5000] and for subcircuits 2 and 5 in the interval [4000, 5000]. For subcircuits 3, 4 and 6, subcircuit 1 becomes the anti-phase synchronization state in the interval [2500, 5000]. In this interval, the size of the cluster for subcircuit 1 is principally 3. Furthermore, subcircuit 1 is synchronized with subcircuits 3, 5 and 6 at the anti-phase and becomes the in-phase synchronization state for subcircuits 2 and 4 in almost all of the interval [5000, 100000]. As the other intervals, the size of the cluster for subcircuit 1 is also principally 3 in this interval. Namely, we can consider that the size of the cluster for subcircuit 1 is easy to become 3 for $N = 6$.

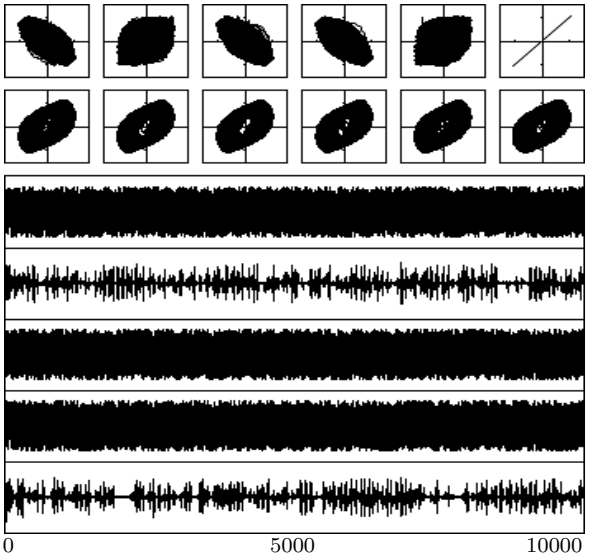

(a) $\alpha = 20.0.$ $\beta = 0.26.$ $\gamma = 0.3.$

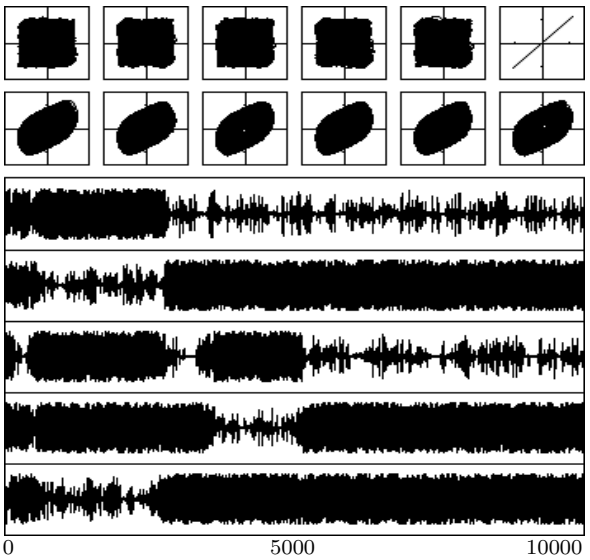

(b) $\alpha = 20.0.$ $\beta = 0.265.$ $\gamma = 0.3.$

Fig. 2 Computer calculated results for $N = 6$. Upper figures: x_1 vs. x_{k+1}. ($x_7 = x_1$.) Middle figures: x_k vs. z_k. Lower figures: τ vs. $x_1 - x_{k+1}$. ($k = 1, 2, 3, 4, 5, 6$.)

4. Statistical Analysis

4.1 Introduction of Phase Variables

In this section, we investigate the clustering phenomenon in detail. First, in order to discriminate whether each subcircuit is synchronized or not, let us define the Poincaré section as $x_1 < 0$ and $z_1 = 0$ Next, we introduce the following independent variables from the discrete data of $x_k(n)$ and $z_k(n)$ on the Poincaré map. The values of $\varphi_k(n)$ correspond to the phase differences between subcircuit 1 and the others. (Note that the argument of the point ($x_1(n)$,$z_1(n)$) is always π, because of the definition of the Poincaré map.) By using the values of $\varphi_k(n)$, we make detailed investigation on the statistical information of the clustering for $N = 6$. In

the statistical analysis, we carried out computer simulations during one hundred thousand iterations of the Poincaré map under the following parameters: $\alpha = 20.0$, $\beta = 0.265$, and $\gamma = 0.3$.

$$\varphi_k(n) = \begin{cases} \pi - \tan^{-1}\dfrac{z_k(n)}{x_k(n)} \\ \quad x_k(n) \geqq 0 \\ -\tan^{-1}\dfrac{z_k(n)}{x_k(n)} \\ \quad x_k(n) < 0 \ \ and \ \ z_k(n) \geqq 0 \\ 2\pi - \tan^{-1}\dfrac{z_k(n)}{x_k(n)} \\ \quad x_k(n) < 0 \ \ and \ \ z_k(n) < 0 \\ (k = 2, 3, 4, 5, 6.) \end{cases} \tag{5}$$

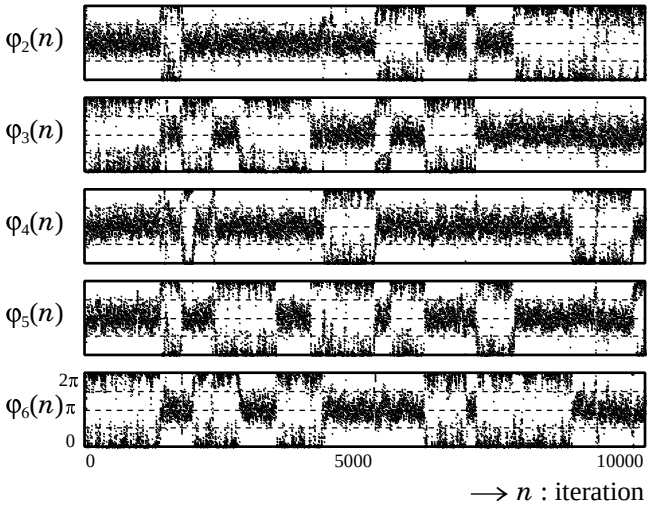

Fig. 3 Time series $\varphi_k(n)$ calculated from the data $x_k(n)$ and $z_k(n)$.

4. 2 Probability distribution of $\varphi_k(n)$

Figure 3 shows the time evolution of $\varphi_k(n)$ calculated from the data $x_k(n)$ and $z_k(n)$. Horizontal axis is the iteration of the Poincaré map. Vertical axis is the phase difference of each subcircuit for subcircuit 1. The switching phenomena occurs at short intervals and the synchronization states change chaotically. Moreover, we can see that subcircuit 1 becomes the in-phase or anti-phase synchronization state for the others with high frequency.

Figure 4 shows the probability distributions of $\varphi_k(n)$. The slots in the horizontal axis of the figure denote the ranges of $\varphi_k(n)$ and are summarized in Tab. 1. We can confirm that all subcircuits become about the same probability distributions. For the reason to become in this way, our circuit model's symmetry can be considered. Furthermore, the probabilities of slots 1, 6, 7, and 12 are larger than the others. We can consider that the slots 1 and 12 correspond to the in-phase states and the slots 6 and 7 correspond to the anti-phase states. This means that each subcircuit becomes the in-phase or anti-phase synchronization state with large probability.

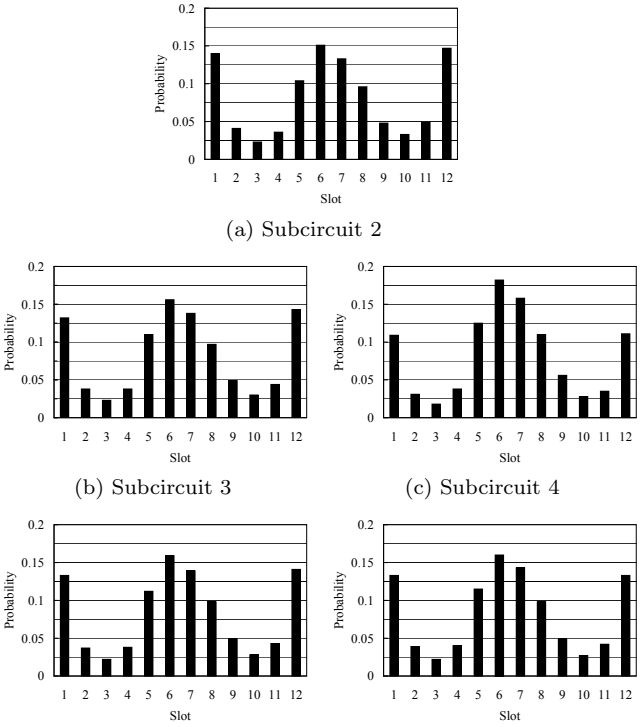

(a) Subcircuit 2

(b) Subcircuit 3

(c) Subcircuit 4

(d) Subcircuit 5

(e) Subcircuit 6

Fig. 4 Probability distributions of $\varphi_k(n)$.

4. 3 Probability distributions of sojourn time

We define that subcircuit 1 is synchronized with subcircuit k if the value of $\varphi_k(n)$ satisfies (6). This definition of the synchronization corresponds to the in-phase synchronization state.

$$-\frac{\pi}{6} < \varphi_k(n) < \frac{\pi}{6} \tag{6}$$

Table 2 shows the probability distribution of cluster sizes for subcircuit 1 are from 1 to 6. "Cluster size = 1" means that subcircuit 1 is not synchronized with the others. Then, "Cluster size = 2" means that subcircuit 1 is synchronized with one of the other five subcircuits and not synchronized with the others. Moreover, "Cluster size = 4" means that subcircuit 1 is synchronized with other three subcircuits. As

Table 1 Ranges of slots in Fig. 4.

Slot	$\varphi_k(n)$	Slot	$\varphi_k(n)$
1	$0 \leqq \varphi_k(n) < \frac{\pi}{6}$	7	$\pi \leqq \varphi_k(n) < \frac{7\pi}{6}$
2	$\frac{\pi}{6} \leqq \varphi_k(n) < \frac{\pi}{3}$	8	$\frac{7\pi}{6} \leqq \varphi_k(n) < \frac{4\pi}{3}$
3	$\frac{\pi}{3} \leqq \varphi_k(n) < \frac{\pi}{2}$	9	$\frac{4\pi}{3} \leqq \varphi_k(n) < \frac{3\pi}{2}$
4	$\frac{\pi}{2} \leqq \varphi_k(n) < \frac{2\pi}{3}$	10	$\frac{3\pi}{2} \leqq \varphi_k(n) < \frac{5\pi}{3}$
5	$\frac{2\pi}{3} \leqq \varphi_k(n) < \frac{5\pi}{6}$	11	$\frac{5\pi}{3} \leqq \varphi_k(n) < \frac{11\pi}{6}$
6	$\frac{5\pi}{6} \leqq \varphi_k(n) < \pi$	12	$\frac{11\pi}{6} \leqq \varphi_k(n) < 2\pi$

Table 2 Probability distribution of cluster sizes for subcircuit 1.

Cluster size	Probability	Cluster size	Probability
1	0.18869	4	0.00020
2	0.30057	5	0.00000
3	0.51054	6	0.00000

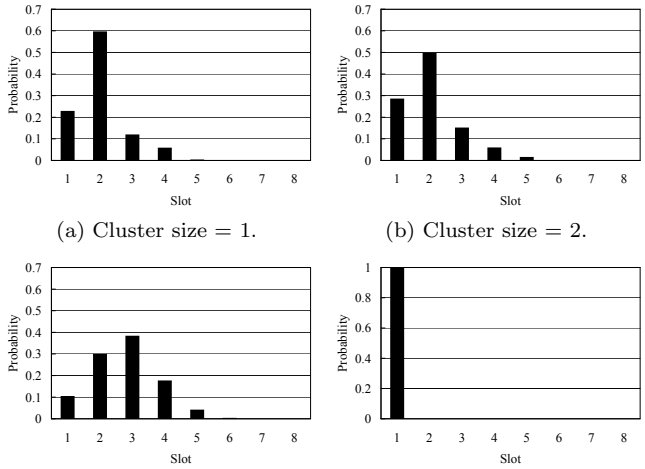

(a) Cluster size = 1. (b) Cluster size = 2.

(c) Cluster size = 3. (d) Cluster size = 4.

Fig. 5 Probability distributions of sojourn time.

Table 3 Ranges of slots in Fig. 5.

Slot	Sojourn time (n)	Slot	Sojourn time (n)
1	1−2	5	21−50
2	3−5	6	51−100
3	6−10	7	101−200
4	11−20	8	201−500

we can see from Tab. 2, the probability of "Cluster size = 3" is the largest and the cluster size hardly becomes more than 4.

While, Fig. 5 shows the probability distributions of sojourn time. The slots in the horizontal axis of the figure denote the ranges of the sojourn time and are summarized in Tab. 3. For example, comparing Fig. 5(c) with Fig. 5(b), the probability distributions of the slots 3, 4, and 5 of "Cluster size = 3" are larger than those of "Cluster size = 2". Furthermore, "Cluster size = 3" disappears within 1 or 2 iterations of the Poincaré map. Clearly, it is confirmed that the larger cluster size is, except the case of "Cluster size = 4", the larger sojourn time is as shown in Fig. 5.

4. 4 Probability distribution of various cluster types.

The probability distribution of specific cluster types for subcircuit 1 is shown in Tab. 4. For example, the probability of the cluster type "1-2-3-4-5-6" is 2.04×10^{-3}. This

Table 4 Probability distribution of specific cluster types for subcircuit 1.

Cluster type	Probability	Cluster type	Probability
1-2-3-4-5-6	0.00204	123-456	0.02845
12-3-4-5-6	0.00189	1234-5-6	0.00001
12-34-5-6	0.00359	1234-56	0.00002
12-34-56	0.00055	12345-6	0.00000
123-4-5-6	0.00467	123456	0.00000
123-45-6	0.01491		

Table 5 Probability distribution of cluster types.

Cluster type	Probability	Cluster type	Probability
1-1-1-1-1-1	0.00204	3-3	0.25662
2-1-1-1-1	0.03006	4-1-1	0.00033
2-2-1-1	0.10004	4-2	0.00048
2-2-2	0.00597	5-1	0.00000
3-1-1-1	0.08581	6	0.00000
3-2-1	0.51865		

Table 6 Probability distribution of the number of clusters.

♯ of clusters	Probability	♯ of clusters	Probability
1	0.00000	4	0.18585
2	0.25710	5	0.03006
3	0.52495	6	0.00204

cluster type means that all subcircuits become asynchronous states and the number of the clusters is 6. This value is relatively large, which is quite interesting in the sense that all subcircuits are connected to the same core. Then, we can confirm that the probability of the cluster type "12-3-4-5-6" is 1.89×10^{-3}. This cluster type means that subcircuit 1 becomes synchronization state for subcircuit 2 and the other subcircuits are not synchronized and the number of the clusters is 5. Moreover, the cluster type "12-34-5-6" means that subcircuit 1 is synchronized with subcircuits 2 and subcircuit 3 is synchronized with subcircuits 4 and subcircuits 5 and 6 independently oscillate and the number of the clusters is 4.

While, the probability distribution of cluster types is shown in Tab. 5. For example, the probability of the cluster type "2-1-1-1-1" is 3.06×10^{-2}. This cluster type means that subcircuit 1 becomes synchronization state for subcircuit 2 and the others are not synchronized each other and the number of the clusters is 5. Furthermore, the cluster type "2-2-1-1" means that subcircuit 1 becomes synchronization state for subcircuit 2 and any two of subcircuits except subcircuit 1 and 2 are synchronized and the others are independently oscillate and the number of the clusters is 4. The probability distribution of the number of clusters is summarized in Tab. 6. This table shows that the number of clusters is easy to become 3 for $N = 6$.

5. Discussion

We considered that the probability distribution of cluster types as shown in Tab. 5 could be calculated only by using the information shown in Tab. 4 as theoretical figures. For example, the probability P_1 of the cluster type "2-1-1-1-1" can be calculated by using the probability of the cluster type "12-3-4-5-6" as follows.

$$P_1 = {}_5C_1 \times 0.00189 = 9.45 \times 10^{-3}. \quad (7)$$

As the same way, the probability P_2 of the cluster type "2-2-1-1" can be calculated by using the probability of the cluster type "12-34-5-6" as follows.

$$P_2 = {}_5C_1 \times {}_4C_2 \times 0.00359 = 0.1077. \quad (8)$$

Moreover, the other various probabilites can be calculated by using the probability information shown in Tab. 4. Those results are summarized in Tab. 7. In addition, the theoretical figure of the probability distribution of the number of clusters is summarized in Tab. 8.

The relative error between statistical data and theoretical figures for cluster types is shown in Tab. 9. We can confirm that the relative errors of the cluster types "2-1-1-1-1", "2-2-2", "3-1-1-1", "4-1-1", "4-2" are quite large. We have to investigate a reason to become in this way in detail. However, if we could calculate various probabilites as shown in Tab. 5 by using a little information as shown in Tab. 4, it would be excellent.

6. Conclusions

In this study, we investigated the clustering phenomenon observed from chaotic circuits coupled by mutual inductors. By carrying out computer calculations, we confirmed the generation of the clustering phenomenon and chaotic changings of the synchronization states for a six subcircuit case. Moreover, we make detailed investigation on the statistical information of the clustering, such as sojourn time of a certain size of clusters, the number of clusters, and so on.

Acknowledgements

This work was partly supported by Yazaki Memorial Foundation for Science and Technology.

Table 7 Theoretical figure of the probability distribution of cluster types.

Cluster type	Probability	Cluster type	Probability
1-1-1-1-1-1	0.00204	3-3	0.28450
2-1-1-1-1	0.00945	4-1-1	0.00010
2-2-1-1	0.10770	4-2	0.00020
2-2-2	0.01650	5-1	0.00000
3-1-1-1	0.04670	6	0.00000
3-2-1	0.44730		

Table 8 Theoretical figure of the probability distribution of the number of clusters.

♯ of clusters	Probability	♯ of clusters	Probability
1	0.00000	4	0.15440
2	0.28470	5	0.00945
3	0.46390	6	0.00204

Table 9 Relative error between statistical data and theoretical figures for cluster types.

Cluster type	Relative error	Cluster type	Relative error
2-1-1-1-1	2.18095	3-2-1	0.15951
2-2-1-1	0.07112	3-3	0.09800
2-2-2	0.63818	4-1-1	2.30000
3-1-1-1	0.83747	4-2	1.40000

References

[1] K. Kaneko, "Clustering, Coding, Switching, Hierarchical Ordering, and Control in a Network of Chaotic Elements," Physica D, vol.41, pp.137-172, 1990.

[2] Y. Maistrenko, O. Popovych and M. Hasler, "On Strong and Weak Chaotic Partial Synchronization," Int. J. Bifurcation Chaos, vol.10, no.1, pp.179-203, 2000.

[3] M. Miyamura, Y. Nishio and A. Ushida, "Clustering in Globally Coupled System of Chaotic Circuits," Proc. of ISCAS'02, vol. 3, pp.57-60, May 2002.

[4] Y. Nishio and A. Ushida, "Chaotic Wandering and its Analysis in Simple Coupled Chaotic Circuits" IEICE Transactions on Fundamentals, vol. E85-A, no. 1, pp. 248-255, Jan. 2002.

[5] Y. Komatsu, Y. Uwate and Y. Nishio, "Synchronization in Chaotic Circuits Coupled by Mutual Inductors," Proc. of NCSP'06, pp.293-296, Mar. 2006.

[6] N. Inaba and S. Mori, "Chaotic Phenomena in Circuits with a Linear Negative Resistance and an Ideal Diode," Proc. of MWSCAS'88, pp.211-214, Aug. 1988.